Nonlinear Dynamics manuscript No.
(will be inserted by the editor)

OGY Method for a Class of Discontinuous Dynamical Systems

Marius-F. Danca

Received: date / Accepted: date

Abstract In this paper we prove that the OGY method to control unstable periodic orbits (UPOs) of continuous-time systems, can be applied to a class of systems discontinuous with respect the state variable, by using a generalized derivative. Because the discontinuous problem may have not classical solutions, the initial value problem is transformed into a set-valued problem via Filippov regularization. The existence of the ingredients necessary to apply OGY method (UPO, Poincaré map and stable and unstable directions) is proved and the numerically implementation is explained. Another possible way analyzed in this paper, is the continuous approximation of the underlying initial value problem, via Cellina's Theorem for differential inclusions. Thus, the problem is approximated by a continuous initial value problem, and the OGY method can be applied as usually.

Keywords Generalized derivative, OGY method, Poincaré map, Filippov regularization, Cellina's Theorem

1 Introduction

In the real word non-smoothness is common. Thus, many physical laws and systems are modeled by a set of first-order differential equations with discontinuous components. Dynamical systems (DS on short) discontinuous with respect to the state variable, appear in a large number of problems from mechanics (dry friction [1] with stick and slip modes [2], impacts [3], oscillating systems with viscous damping [4], elasto-plasticity [5], vibrations [6], braking processes with locking phases [7]), electrical (chaotic) circuits [8], networks with switches [9], power electronics [10]), but also in theory of automatic and optimal control [11], optimization [12,13], games theory [14], uncertain systems [15], walking machines [16], biological and physiological systems [17] and everywhere non-smooth characteristics are used to represent switches (see also the references in [18,12,19–21]).

In practical examples the discontinuity may appears because of switch like functions which (e.g. signum, Heaviside function-also known as the "unit step function", maximum etc.).

Continuous our discontinuous, most nonlinear systems behave chaotic under certain circumstances. Therefore, the desire to control the chaotic evolutions are legitimate and the *chaos control* (called sometimes *chaos stabilization* or *chaos suppression*) is an important topic of chaos theory and a key challenge in many areas of applied an theoretical science.

The chaos control methods can be classified as follows

- Methods with slightly perturbations of a system parameter, the most known method being OGY, named for Ott, Gebogi and Yorke in the seminal work [22], which forces some trajectory to reach a particular unstable periodic orbit (UPO) via the linearization of a Poincaré map;
- Methods with small perturbations in the system variables in the form of instantaneous pulses (see e.g. the method proposed by Güemez and Matías

Marius-F. Danca
Dept. of Mathematics and Computer Science
Avram Iancu University
400380, Cluj-Napoca, Romania

and
Romanian Institute of Science and Technology,
400487 Cluj-Napoca, Romania
E-mail: danca@rist.ro

in [23], [24] for discrete and continuous DS, or [25] discontinuous DS).

While the first algorithms are useful in the cases when some system parameters are accessible, the second class of methods are useful in the cases when the parameters are unaccessible, namely in the cases of certain chemical, biological electrical circuits etc.

In this paper we prove that the OGY method can be applied not only for continuous systems, but also for a class of discontinuous DS modeled by the following Initial Value Problem (IVP)

$$\dot{x} = f(x) := g(x) + As(x),\ x(0) = x_0,\ t \in I = [0, \infty), \tag{1}$$

with$f, g : \mathbb{R}^n \to \mathbb{R}^n$, g of class $C^1(\mathbb{R}^n)$, $A = (a_{i,j})_{n \times n}$ a real constant matrix and the vector function $s : \mathbb{R}^n \to \mathbb{R}^n$ given by

$$s(x) = \begin{pmatrix} sgn(x_1) \\ \vdots \\ sgn(x_n) \end{pmatrix}.$$

Examples of systems modeled by the IVP (1) can be found in most of the above mentioned applications.

Remark 1 The considered systems, modeled by the IVP (1) are time-continuous and discontinuous with respect to the state variables.

The paper is structured as structured as follows: Section 2 contains the basic necessary notions and results related to the existence and numerical calculation of solutions of the IVP (1) and Section 3 presents shortly the continuous variant of the OGY method and proves the implementation of the OGY method to discontinuous systems of class (1).

2 Preliminary notions and results

Notation 1 *The null set of the discontinuity of f (points where the sign functions vanish) will be denoted by $\mathscr{M}$ and the continuity domain by $\mathscr{C}$.*

Due to the *sgn* functions, the continuity domain consists in a finite number of open regions $\mathscr{C}_i$ (denoted sometimes by $\mathscr{C}^{\pm}$ in order to simplify the exposure) which verify $\mathscr{C} = \bigcup \mathscr{C}_i = \mathbb{R}^n \backslash \mathscr{M}$. Thus, the state space $\mathbb{R}^n$ is split into $\mathscr{C}_i$ by one hyperplane or by the intersection of several hyperplanes called *switching surfaces* defined by the *indicator function* $H : \mathbb{R}^n \to \mathbb{R}^n$. Due to the *sgn* functions, the switching hyperplanes Σ_k, have the equations $H(x) = 0$, i.e. $x^k = 0$, $k \in \{1, 2, ..., n\}$, where x^k is the k-th component of the state vector $x = (x^1, x^2, ..., x^n) \in \mathbb{R}^n$. In the continuity domains $\mathscr{C}^{\pm}$, $sgn(H(x)) = \pm 1$.

Example 1 Let consider

$$f(x) = x + sgn(x).$$

Here $g(x) = x$, $M = \{0\}$, and the indicator function $H(x) := x = 0$ divides $\mathbb{R}$ into the subspaces $\mathscr{C}^- = (-\infty, 0)$ and $\mathscr{C}^+ = (0, \infty)$. In $\mathscr{C}^-$, $H(x) < 0$ and in $\mathscr{C}^+$, $H(x) > 0$.

Notation 2 *As known, the terms* trajectory, orbit, *and* flow *can be considered to be similar, but they outline different aspects of the same phenomenon. In this paper we shall call* trajectory *and* orbit *the path defining the dynamics of continuous time systems (continuous or discontinuous with respect to the state variable) and discrete systems respectively.*

The vector field of an ODE defines a *flow* which transforms an initial condition x_0 into some state $x(t)$ and time $t \in I$. Except the case of the consecrated term Poincaré *map*, we shall use the term *function*.

The notions presented next (which can be found in the comprehensive works [26,27]) will be considered here, in the most encountered space in applications, the Euclidean space $\mathbb{R}^n$.

Let $F : \mathbb{R}^n \rightrightarrows \mathbb{R}^n$ a set-valued function (a relation which to each input associates at least one output element).

Definition 3 A set-valued map F is characterized by its $Graph(F)$, the subset of the product space $\mathbb{R}^n \times \mathbb{R}^n$ defined by

$$Graph(F) := (x, y) \in \mathbb{R}^n \times \mathbb{R}^n | y \in F(x).$$

We shall say that $F(x)$ is the image or the value of F at x.

Remark 2 A set-valued map satisfies a property P of a subset (for instance, closed, convex, etc.) if and only if his graph satisfies it.

Definition 4 We say that F is *upper-semicontinuous* (USC) at $x^0 \in \mathbb{R}^n$ if for any open N containing $F(x^0)$, there exists a neighborhood M of x^0 such that $F(M) \subset N$.

Definition 5 A *selection* of a given set-valued function F is a single-valued function $h : \mathbb{R}^n \to \mathbb{R}^n$ satisfying $h(x) \in F(x)$, for all $x \in \mathbb{R}^n$.

In practical examples of discontinuous systems, when selections are used, it is sufficient to determine the selections only in some neighborhoods of $\mathscr{M}$ points (Figure 1).

In order to deal with OGY's method, the derivative is an essential notion. Let consider the discontinuous function f defined in (1). Because the classical notion of derivatives at the discontinuity points of f cannot be used here, a new concept of derivative for our class of functions (which uses the classical derivative notion at the continuity points) was introduced in [28].

Definition 6 Let f be differentiable on some open domain $\mathscr{C} \subset \mathbb{R}^n$. We say that f is *generalized differentiable* at $x^* \in \mathbb{R}^n$ if the following limit exists and is finite

$$\mathscr{D}_x f(x^*) := \lim_{x \to x^*} D_x f(x), \quad x \in \mathscr{C}, \tag{2}$$

where D_x is the classical Jacobian matrix. $\mathscr{D}_x$ will be called the *generalized (Jacobi) derivative*.

We say that f is *generalized differentiable on* $\mathbb{R}^n$ if it is so at every $x^* \in \mathbb{R}^n$.

Notation 7 *The class of functions f having generalized derivative on $\mathbb{R}^n$ will be denoted by $\mathscr{C}^1(\mathbb{R}^n)$.*

The following useful result can be easily checked [28].

Proposition 1 *Let consider the IVP (1) with $g \in C^1(\mathbb{R}^n)$. Then, $f \in \mathscr{C}^1(\mathbb{R}^n)$ and*

$$\mathscr{D}_x f(x) = D_x g(x), \quad x \in \mathbb{R}^n. \tag{3}$$

For Example (1), $g(x) = x$ is a $C^1(\mathbb{R})$ function, $\mathscr{M} = \{0\}, \mathscr{C}_1 = (-\infty, o), \mathscr{C}_2 = (0, \infty)$ and, at $x = 0$, we have $\mathscr{D}_x f(0) = \lim_{x \to 0} f'(x) = 1$ and therefore $\mathscr{D} f(x) = 1$ for all $x \in \mathbb{R}$.

2.1 Solutions to IVP (1)

In the points of $\mathscr{M}$, the IVP (1) may have not sense and may have not any solutions in the classical sense. For example the IVP

$$\dot{x} = 2 - 3sgn(x), \; x(0) = x_0 \tag{4}$$

with discontinuous right-hand side (see Figure 2 a) has for $x_0 \neq 0$, the classical solutions

$$x(t) = \begin{cases} 5t + x_0, \text{ for } x_0 < 0, \\ -t + x_0, \text{ for } x_0 > 0, \end{cases} \tag{5}$$

while for $x_0 = 0$ there are no classical solutions since $x(t) = 0$ does not verify the equation. In other words, for $x_0 \neq 0$, the solutions tend to the line $x = 0$ but they cannot continue along this line (Figure 2 c).

A common device to obtain a precise mathematical setup of this problem is to replace the single-valued underlying IVP with a set-valued one. The obtained IVP can be handled via differential inclusions (DI) theory (see e.g. [26] or [29]). Thus, using some regularization procedure (e.g. the so called Filippov regularization [29]), the discontinuous IVP is transformed into a set-valued Cauchy problem

$$\dot{x} \in F(x), \qquad x(0) = x_0, \quad \textit{for a. a. } t \in I, \tag{6}$$

where, instead of a differential equation, we have a DI.

The Filippov regularization [29] defines $F(x)$ as follows

$$F(x) = co \lim_{x' \to x} f(x'), \tag{7}$$

where co is the convex hull and $\lim_{x' \to x} f(x')$ is the set of all limits of all convergent sequences $\{f(x_k)\}$ with $\{x_k\} \to x$.

For $x \in \mathscr{M}$, $F(x)$ is a set, while for $x \in \mathscr{C}$, $F(x)$ consists in a single point, $f(x)$. For instance, the set-valued form of sgn function, which will be used to transform the IVP (1) into a convex set-valued problem, is

$$Sgn(x) = \begin{cases} \{-1\}, & x < 0, \\ [-1, 1], & x = 0, \\ \{+1\}, & x > 0. \end{cases} \tag{8}$$

Thus, $sgn(0)$ is replaced with the whole interval $[-1, 1]$, connecting thus the points -1 and $+1$.

For example, after Filippov regularization, (4) becomes

$$\dot{x} \in 2 - 3Sgn(x) \tag{9}$$

which, for $x = 0$, has the right-hand side the set $[-1, 5]$ (see Figure 2 b). One can consider that the right-hand side is actually set-valued only in $x = 0$, while for $x \neq 0$ the right-hand side being a single-valued function.

Applying the Filippov regularization to the IVP (1) one obtains

$$\dot{x} \in F(x) := f(x) + AS(x), \quad x(0) = x_0, \quad \textit{for a.a. } t \in I, \tag{10}$$

where $S(x) = (Sgn(x_1), \ldots, Sgn(x_n))^T$

It is easy to see that Sgn function (8) is USC and therefore the right-hand side of (10) is USC too [30].

A set-valued IVP may have (several) *generalized (Filippov) solutions* which leads to the notion of solutions to IVP (1).

Definition 8 A *generalized (Filippov) solution* to (1) is an absolutely continuous function $x(\cdot) : [0,\infty) \longrightarrow \mathbb{R}$, satisfying (10) for a. a. $t \in [0,\infty)$.

Remark 3

i) The existence (Péano) theorem, presented in many works (e.g. [26,27,29,31]), ensures the existence of solutions for a DI if his right-hand side is a Péano function, i.e. USC with nonempty closed and convex values. As proved in the mentioned texts, F obtained with the Filippov regularization (7) enjoys these properties.

ii) In [30] beside the necessary conditions for uniqueness, it is proved that the right-hand side of the IVP (1) is a Péano function and the IVP (1) admits solutions.

For example, after the regularization, the obtained set-valued IVP (9) has a generalized solution which is, for $x_0 < 0$ (Figure 2 d)

$$x(t) = \begin{cases} 5t + x_0, \text{ for } t < -x_0/5, \\ 0, \text{ for } t \geq -x_0/5, \end{cases}$$

and, for $x_0 > 0$

$$x(t) = \begin{cases} -t + x_0, \text{ for } t < x_0, \\ 0, \text{ for } t \geq x_0, \end{cases}$$

Notation 9 *If $x(t)$ is a solution of the IVP (1), let the flow $\varphi^t(\cdot,p) : \mathbb{R} \times \mathbb{R}^n \to \mathbb{R}^n$, $t \in I = [0,\infty)$ which satisfies $\varphi^t(x_0,p) = x(t)$, $\frac{d}{dt}\varphi^t(x_0,p) \in F(\varphi^t(x_0,p)) = x(t)$ a.a. in I, and $\varphi^0(x_0,p) = x_0$, with F defined in (10). $\varphi^0 = I_n$, meaning that the flow at $t = 0$ starts at the initial condition x_0.*

Remark 4 Even the flow φ^t of the IVP (1) is composed by several concatenated flows φ_i^t defined in each subregion of $\mathscr{C}$, φ^t is continuous, and may contains corners on the discontinuity surfaces. Thus, supposing that Σ determines two continuity domains $\mathscr{C}^{\pm}$, the trajectory may enter Σ with the tangential direction f^- imposed by the vector field defined in $\mathscr{C}^-$ at the entering point M, and exits along a different tangential direction f^+ defined by the field in $\mathscr{C}^+$ in the exit point N (Figure 3).

2.2 Numerical integration of IVP (6)

Let us first consider a general autonomous set-valued problem $\dot{x} \in F(x)$ on $I = [t_0,T]$, with F a Péano set-valued function (Remark 3 i) with F defined by (7).

A numerical method for DI consists in replacing the DI on I, with a sequence of discrete inclusions on a sequence of girds

$$t_0 < t_1 < ... < t_N = T,$$

where $N \in \mathbb{N}' \subset \mathbb{N}$ and the step-size $h = (T - t_0)/N = t_j - t_{j-1}$, for $j = 1, ..., N$.

For the sake of simplicity, next we consider the simplest numerical method to integrate DIs, the explicit Euler method (other explicit or implicit methods for DI can be found e.g. in [31] or [32]). Let consider (6) with $y_0 = x_0$. Then, the sequence $\{y_n\}$ which approximates the solution in the points t_n is

$$y_{j+1} \in y_j + hF(y_j), \quad j = 0, 1, ..., N-1. \tag{11}$$

As a solution of the discrete DI (11) it is convenient to consider any continuous piece-wise linear function $y^N : I \to \mathbb{R}^n$ [31]

$$y^N(t) = y_j + \frac{1}{h}(t - t_j)(y_{j+1} - y_j),$$
$$t_j \leq t \leq t_{j+1}, \quad j = 0, 1, ..., N.$$

In general, a set-valued function admits infinitely many values, or selections. Therefore, the key of solving (11) is the choice of selections which means choice of selecting points from the set-valued F. Thus, the selection can be chosen by some minimization criterion, or just by some random choice of selection in the grid points (see [31,32]). For example in the set-valued function $[-1, 5]$ which appears in the example (9), for derivative one can choose randomly a value inside this interval.

There is a rich literature dealing with the Euler convergence theorem for DI (see e.g. [29, Theorem 1, pp.77]; [26, Lemma 1 pp. 99], or [31,32]). In these works it is showed that (11) with F a Péano function has a convergent subsequence in $[t_0,T]$ to some trajectory of (6).

For our problem (1), the solutions can be calculated classically in $\mathscr{C}$ (as ODE), and with a numerical scheme for DI in $\mathscr{M}$. Thus, numerically, when a trajectory arriving from one of the continuity domains (e.g. $\mathscr{C}^-$ in Figure 3), meets a discontinuity surface, it needs a finite, relatively small time interval to traverse it (from points M to N). The two underlying time moments, t_1 and t_2, when the trajectory enters and exits the surface respectively, can be found with some so called *stopping procedures*, e.g. when the indicator function H changes his sign. In order to obtain a more accurate intersection with the discontinuity surface (implicitly reduce the time interval $[t_1^{'}, t_2^{'}] \subset [t_1, t_2]$), one can use some numerical method to find the zero of the function $H(x) = 0$, after the moment when it changes the sign. In the time interval $[t_1, t_2]$ (or $[t_1^{'}, t_2^{'}]$), which has the length less than the integration step size (which can be the same in $\mathscr{C}$ and $\mathscr{M}$ if one use a fixed step-size method), the IVP is integrated as a DI, as mentioned before.

Computer tests show that using highly consistent methods to avoid the typical corners in $\mathscr{M}$ points (Figures 3, and 4), it is not worthwhile, except in continuous domain $\mathscr{C}$ (see e.g. [31]).

Other ways to solve this kind of set-valued IVPs, used especially in engineering applications, can be found in e.g. [1].

3 OGY for IVP (1)

3.1 OGY for continuous systems

First, we need to recall briefly, the OGY method for continuous chaotic systems. Being described in many works (see e.g. the references in [53]) only the main steps will be pointed out.

The original variant of the OGY method is effective only for lower-dimensional chaotic systems[1], because for higher dimensions, when the Jacobian at some fixed point may have complex or multiple eigenvalues, the construction of stable and unstable manifolds is a technical challenge. Therefore let us consider the three-dimensional case of continuous chaotic systems modeled by

$$\dot{x} = f(x, p) \tag{12}$$

where $f : \mathbb{R}^3 \to \mathbb{R}^3$ is a smooth function and $p \in \mathbb{R}$.

Suppose the system (12) admits, for the nominal parameter value p_0, an UPO of period N, denoted Γ, with points y_n, $n = 0, 1, 2, ..., N$, $y_N = y_0$. Γ can be determined numerically with the so called PIM-triple method [39].

Let an suitable bidimensional Poincaré section, Σ (usually $n-1$-dimensional hyperplane for autonomous systems and n-dimensional for periodically driven systems), chosen transversally to Γ (i.e. not tangent to Γ) such that Γ intersect Σ in the same sense as previous intersection (intersections in either senses, related sometimes as *first-return map*, are not considered here).

Due to the periodicity, Γ will intersect Σ in N points. In order to simplify the exposure, without loss of generality, next one consider only one of the points where Γ pierces Σ, namely y_Γ, which is a saddle. Since y_Γ is arbitrarily, one can consider that each point on Γ can be considered a saddle and the stability properties of Γ are independent of the cross section Σ.

OGY method implies one want to approximate Γ by a stable trajectory denoted hereafter by Θ with points $\{x_n\}$, $n = 0, 1, 2, ...$

[1] Meanwhile, several modified variants for higher-order systems were developed.

Starting from a randomly chosen initial condition x_0, due to mixing property of the attractor (initial conditions get spread over the attractor), Θ will eventually come sufficiently close to Γ, i.e. some point x_n arrives close to y_Γ. This is the moment when, actually, the OGY method effectively begin.

As known, the Poincaré map reduces the study of the stability of a periodic orbit of the starting continuous system, to the study of the stability of a fixed point of a discrete system in the entire Σ or in some neighborhood of y_Γ. Therefore, in order to describe the OGY method, we can focus exclusively on Σ points where a smooth recursive Poincaré map $P : \Sigma \to \Sigma$ can be defined

$$x_{n+1} = P(x_n, p), \quad n = 0, 1, ... \tag{13}$$

Therefore, under P, the unstable periodic fixed point y_Γ verifies $y_\Gamma = P(y_\Gamma, p_0)$. When Θ pierces Σ in some point x_n sufficiently close to y_Γ (i.e. belongs to some neighborhood U of x_Γ), the control parameter p is adjusted with small carefully chosen perturbations, in such a way that x_n remains, in the next step, close to y_Γ. For this purpose, we require to control the unstable direction of x_n in U i.e. force x_n to fall on the stable direction. The stability of y_Γ is described by the eigenvalues of the Jacobian of P evaluated at y_Γ.

If one denote the perturbation by $\Delta p = |p - p_0|$, p will be perturbed every time when x_n enters U with the following quantity, obtained via linearization of the Poincaré map

$$\Delta p = \frac{A(x_n - y_\Gamma)\omega_u}{-Bw_u} \tag{14}$$

where $A = D_x F(x, p)|_{x=y_\Gamma, p=p_0}$ is the 2×2 Jacobian of F evaluated at y_Γ for $p = p_0$. The column vector $B = D_p F(x, p)|_{x=y_\Gamma, p=p_0}$ measures the sensitivity of the system to parameter perturbations, and w_u is the unstable contravariant vector.

If $|\Delta p| > \delta$, where δ is the required maximum parameter perturbation, we set $\Delta p = 0$, i.e. p is set to p_0 meaning that Θ still has not entered yet in U.

Finally, the orbit $\{x_n\}$ will become an stable orbit close to UPO, and one can consider that the reference unstable orbit UPO was stabilized.

Obviously, without control, Θ will diverge from the reference UPO.

The success key of OGY method is the ergodicity property.

Summarizing, in order to apply OGY method, the following elements have to be determined: a) UPO; b) Poincaré section (map); c) the stable and unstable directions and the underlying contravariant vectors in y_Γ.

3.2 OGY for discontinuous systems

In this section we prove that, under some assumptions, the OGY method can be applied to the IVP (1). For this purpose, we will check each steps required by OGY method.

For the considered UPO, Γ, assume the underlying flow $\varphi^t(\cdot, p_0)$, $t \in I = [0, \infty)$ and $x = (x^1, x^2, x^3) \in \mathbb{R}^3$, has the period time T i.e. $\varphi^{t+T}(x, p_0) = \varphi^t(x, p_0)$, for all $t \in I$ and $x \in \Gamma$[2].

Let next consider the following assumptions
(**H1**) $x_0 \notin \mathscr{M}$ and the solution starting from some x_0, crosses transversal the switching surfaces and not stay on it (no sliding mode);
(**H2**) The Poincaré section, (usually $n-1$-dimensional hyperplane for autonomous systems and n-dimensional for periodically driven systems), here a bi-dimensional plane, is chosen such that his intersection point with the UPO, y_Γ, does not belong to the switching plane(s), i.e. $y_\Gamma \notin \mathscr{M}$.

Remark 5 i) The dynamics on the switching surfaces are treated e.g. in [29,35,36,34] or [37]

ii) Even Assmuption (**H2**) looks restrictive, as in the most practical examples modeled mathematically by IVP (1), there exists a single switching plane $x^i = 0$, for $i \in \{1, 2, 3\}$ (i.e. only a single element $a_{i,j}$ of A in IVP (1) is not zero). Therefore, as usual for continuous systems, the Poincaré section could be the plane $x^i = a$ (see Figure 4) for some $i \in \{1, 2, 3\}$ and with $a \neq 0$. Anyway, the case of two or three switching surfaces can be also easily handled (see [38]).

– **UPO**

Existence
Existence of Γ in systems modeled by (1) is obvious since the underlying chaotic attractors have the key property to have a dense set of unstable periodic orbits.

Numerical determination
Γ can be determined numerically with the so called PIM (Proper Interior Maximum)-triple method proposed by Nusse and Yorke [39] (see also e.g. [47–49]) in the same way as for continuous systems. The method detects and computes chaotic saddles if the unstable dimension is one. Actually it sets out to find a long trajectory near the chaotic saddle and it is based on the fact that trajectories starting close to the stable manifold of the saddle, remains for a long time in its vicinity.
Briefly, let consider the planar diffeomorphism $P : \mathbb{R}^2 \to \mathbb{R}^2$. One begins by taking an interval $L^1 = AB$ in a restraining region, such that it intersects the stable manifold of the saddle. On this interval, one chose next (say 30 [39]) initial points uniformly distributed and one measure their time to leave the region (life or escape time). Among these points one can find an interior point M_1^1 (i.e. M_1^1 is between A and B) which has the longest life time. If one consider his two neighborhoods, A^1 and B^1, one have a new segment A^1B^1 and the three points (A^1, M_1^1, B^1), with M_1^1 the proper interior maximum. This triplet is the PIM-triple. It is expected that A^1 and B^1 lie on two different sides of a branch of the stable manifold. Next step one applies the method on the line segment A^1B^1 and one obtains the PIM-triple (A^2, M_1^2, B^2) with M_2^1 the proper maximum, and so on until this refining procedure produces a shorter segment L_1 of length less than a prescribed precision (e.g. 10^{-9} as described in the mentioned references). Then one consider that one obtained the refinement of the first PIM-tripple segment L^1 (whose length become now less than 10^{-9}) with the proper maximum $\overline{M_1}$. Next, one iterate under P the ends of L^1 and, by applying the above refinement procedure, one obtains the refined segment L_2 with $\overline{M_2}$ the interior of PIM-triple, and so on until one obtains a sequence of PIM-triple intervals $\{L_n\}$ each of length less than 10^{-9}.
The coordinates of midpoints $\{\overline{M_n}\}$ of the $\{L_n\}$, verify $x_{n+1} = P(x_n) + \varepsilon$, with ε of order of 10^{-9}, and are the required points of the an unstable trajectory on the chaotic saddle.
In the considered region, these points approach the stable manifold and, in the same time, move away from the unstable manifold.
As we shall see next, due to the fact that the chosen Poincaré map for our systems (1) is a local diffeomorphim in some small region, UPO can be determined by the above algorithm.

– **Poincaré map**

Existence
Despite the facts that: the existence of a Poincaré map is far from obvious; there are many cases when it simply does not exist; the Poincaré maps are in general discontinuous even for the case of continuous DS, and there may be regions of the flow where P is undefined, i.e. points in such a region never return to Σ. However, under assumptions (H1)-(H2) one can find a suitable transversally Poioncaré section,

[2] For autonomous systems, like those modeled by (1), T is considered to be the smallest time τ, for which a trajectory starting at a point x on the Poincaré surface, pierces again the surface in a small neighborhood of x [33].

such that Γ intersects Σ in y_Γ, in the same sense as previous intersection. The transversal condition in y_Γ is $\langle n_{y_\Gamma}, f(y_\Gamma)\rangle \neq 0$, where n_{y_Γ} is the normal at y_Γ, $\langle\cdot\rangle$ being the inner product.

Remark 6 It is to mention that the simplest failure of the transversality condition may change dramatically the geometric properties of the trajectories.

By the implicit function theorem (which applies under assumption (H1)-(H2) and taking account on Proposition 1), there exists an open neighborhood $U \subset \Sigma$ of y_Γ such that the trajectories starting at U, return to Σ in a time which is close to T. In U one can find a unique Poincaré map of subsequent crossings of Σ, $P : U \times \mathbb{R} \to \Sigma$, $P(x,p) = \varphi^T(x,p)$, $x \in \Sigma$ (see e.g. [33])[3] which is at least a local difeomorphism, the differentiability being ensured by the transversality ([33,41]). P is recursive

$$x_{n+1} = P(x_n, p). \tag{15}$$

and the fixed point y_Γ verifies $P(y_\Gamma, p_0) = \varphi^T(y_\Gamma, p_0) = y_\Gamma$, i.e. the trajectory starting from y_Γ will hit again Σ in approximately T seconds. In other words, one can say that the fixed point of P, y_Γ, is an initial condition for Γ.

Numerical calculation
In the practical problems, the Poncaré maps can be found only numerically. For this purpose we have to solve the system of differential equations, and also detect the fixed points.
Let consider the common choice (see Remark 5) $\Sigma = \{x \in \mathbb{R}^3 | x^k = a\}$, $k \in \{1,2,3\}$. Let Θ, with some initial condition x_0, the trajectory which has to be a stable one close to Γ. For this purpose we have to integrate (1) following the way indicated in Subsection 2.2 until the trajectory arrives, for some n, closely to Σ, i.e. two consecutive points of the trajectory lie on different side of Σ. Next, the intersection point will be found as the zero of the function $x_n^k - a$, where x_n^k is one of the components of the Θ sequence $\{(x_n^1, x_n^2, x_n^3)\}$, obtained by using, for example, the Newton method. As mentioned before, special attention must be payed to choose only the returns on Σ which have the same sense like the previous one (i.e. the trajectory enters Σ from the space e.g. $x^k - a < 0$ to $x^k - a > 0$) (Figure 5). At the end of the algorithm, one obtains a point of the Poincaré map. Then, the algorithm repeats to find the next point map and so on.

The stopping procedure used to find the section was presented first by Hénon in [42] and improved and generalized in e.g. [43] and [44] (see also [33]).

– **Stable and unstable directions e_u and e_s**

Existence
Since we saw the Poincaré map (15) is a locally diffeomorphism, the Stable Manifold Theorem guarantees the existence of stable and unstable local directions e_u and e_s [45] which are constructed via the eigenvalues of the Jacobian of the Poincaré map, called also *monodromy matrix* $M(t)$, evaluated at y_Γ. In our considered case $\mathbb{R}^3$, the stable and unstable directions are one-dimensional, fact which allows the use of the PIM-triple algorithm to find UPO.
As known, the monodromy matrix, $M(T)$, is the fundamental matrix solution $\Phi(t)$ of the IVP (1), after the period T, $M(T) = \Phi(T)$, relating the states of the system at time t and $t+T$. The fundamental matrix solution Φ is solution of the the variational problem for the linearized equation about Γ

$$\dot{\Phi} = \mathscr{D}_x f(x_\Gamma)\Phi, \quad \Phi(0) = I_n. \tag{16}$$

where D_x has been replaced with the generalized derivative $\mathscr{D}_x$. Under considered assumptions, the monodromy matrix can be calculated such as for continuous systems. Thus, let us consider a discontinuous system with a single switching surface $\Sigma = \{x \in \mathbb{R}^3 | x^i = 0\}$, which splits $\mathbb{R}^3$ in the continuity domains $\mathscr{C}^\pm$, and having the form

$$\dot{x} = \begin{cases} f_1(x), \text{ for } x \in \mathscr{C}^-, \\ f_2(x), \text{ for } x \in \mathscr{C}^+, \end{cases}$$

with $x(0) = x_0 \in \mathscr{C}^-$. Then, if one consider the flow cross Σ, in $x \in \mathscr{C}^-$ we have the fundamental matrix solution Φ_1 and, after the trajectory pierces Σ, for $x \in \mathscr{C}^+$, the fundamental matrix solution Φ_2. Since $\mathscr{D}_x f_1(x) = \mathscr{D}_x f_2(x)$, following (16), one obtains $\Phi_1 = \Phi_2$ for $t \in I$ and, therefore, equation (16) is valid for our class of problems.
$\Phi(T)$ exhibits the eigenvalues (characteristic Floquet multipliers) $1, \lambda_1, \lambda_2, ..., \lambda_{n-1}$[4].

Remark 7 As mentioned before, for higher-dimensional Poincaré maps ($n > 2$) there may be several stable and unstable directions which make the algorithm cumbersome.

[3] The Poincaré map is defined on the entire section Σ only if the underlying system is non-autonomous and presents periodically forced vector field (see [40]).

[4] The reason of appearance of the Floquet multiplier 1 in the eigenvalues spectrum relies on geometric reasons. The reminder multipliers are identical to the eigenvalues of the linearization of the Poincaré map. ([46] Theorem 1.6, p. 30).

Numerical calculation
At the saddle y_Γ, the planar linear map $\Phi(T)$ has only two eigenvalues: a stable eigenvalue λ_s and an unstable eigenvalue λ_s which satisfy $|\lambda_s| < 1$ and $|\lambda_u| > 1$.
To calculate these stable and unstable directions, e_s and e_u, one can use the algorithm presented in [47] (also we refer to [34,50,51,33]).
Around y_Γ, one can consider a circle. The system dynamics will transform this circle into an ellipse. The unstable direction is the larger radius of the ellipse, while the smaller is the stable direction.
Since the the two eigenvalues exist and cannot be zero, the monodromy matrix M is invertible and therefore there exists P^{-1}.
First, y_Γ is iterated forward N times under P obtaining the trajectory: $P(x_\Gamma), P^2(x_\Gamma), ..., P^N(x_\Gamma)$. Next, we place a circle of arbitrarily radius at $P^N(x_\Gamma)$. Iterating backward the circle under P^{-1}, it deforms becoming in $P^{n-1}(x_\Gamma)$ into an ellipse. Continuing this process, the ellipse becomes very thin in y_Γ, his major axis being the stable direction.
To find the unstable direction on y_Γ, one iterate N times y_Γ backward with P^{-1}, i.e. $P^{-1}(x_\Gamma), P^{-2}(x_\Gamma)$, $..., P^{-(n-1)}(x_\Gamma), P^{-N}(x_\Gamma)$. There, one place the circle and one iterate it forward N times. Finally, the largest axis is the unstable direction.
In practice, for the sake of simplicity, instead a circle we can take a unit vector and iterate it forward and backward.
In the Euclidean plane, the stable and unstable directions, e_s and e_u, and the contravariant basis, satisfy in each point the conditions $w_u e_u = w_s e_u = 1$ and $w_u e_s = w_s e_u = 0$, wherefrom one can calculate w_u necessary in relation (14).

Thus, the existence of all the ingredients necessary for OGY method have been proved. Summarizing, one can enounce the following property

Proposition 2 *Let the discontinuous system (1) with g of $C^1(\mathbb{R})$ class and having an UPO Γ. Then the correction (14) is well defined and Γ can be approximated by a stable periodic orbit with the OGY method.*

3.3 OGY for continuous approximated system

Another approach of stabilizing the UPO is to approximate continuously the set-valued of the right-hand side of (1) in some neighborhood.

As we saw in Subsection 2, to solve the discontinuous IVP (1), the single-valued problem can be transformed into the set-valued IVP (10). Because the right-hand side is a convex multifunction, the following approximation theorem (Cellina's Theorem) can be applied

Theorem 1 ***(Approximate Selection Theorem [26, Theorem 1, pp.84])*** *Let F a convex USC set-valued function. Then for every $\varepsilon > 0$ there exists a locally Lipschitz function $h_\varepsilon : X \to Y$ such that*

$$Graph(h_\varepsilon) \subset B(Graph(F), \varepsilon),$$

and for every $x \in X$, $f_\varepsilon(x)$ belongs to the convex hull of the image of F.

In practice, one of the most utilized selections is the real valued sigmoid function. For *sgn* functions utilized in our IVP (1) the sigmoid function is $h_\varepsilon : U \to \mathbb{R}$

$$h_\varepsilon(x) = \frac{2\alpha}{1 + e^{-x/\varepsilon}} - \beta,$$

where U is a neighborhood of a discontinuity point and α and β are to be found from continuity imposed at the neighborhood frontier of U (Figure 1).

It is easy to see that the set-valued map of the right-hand side of (10) is convex and USC. Therefore Theorem 1 applies and we can find a Lipschitz selection, which approximates continuously the discontinuous IVP (1) in ε-neighborhoods of M points.

Another continuous and even smooth approximation can be realized via three-order polynomials (polynomials are Lipschitz on finite intervals) $p_\varepsilon : \mathbb{R} \mapsto \mathbb{R}$, $p_\varepsilon(x) = a_1x^3 + a_2x^2 + a_3x + a_4$, where $a_i \in \mathbb{R}$ are to be found from continuity and smoothness conditions imposed at $\pm\varepsilon$ [52].

For instance, let us consider the simplest two-dimensional model Coulomb friction [5]

$$\begin{aligned} \dot{x}_1 &= x_2, \\ \dot{x}_2 &= -x_1 - sgn(x_2), \end{aligned} \tag{17}$$

with $g(x) = (x_2, -x_1)^T$, $A = \begin{pmatrix} 0 & 0 \\ 0 & -1 \end{pmatrix}$, $s(x) = (sgn(x_1), sgn(x_2)^T$, $M = \{(x_1, 0) \in \mathbb{R}^2 | x_1 \in \mathbb{R}\}$, $\mathscr{C} = \{(x_1, x_2) \in \mathbb{R}^2 |\ x_2 \neq 0\}$ (see Figure 6 a where the graph of the second component of f is plotted). After Filippov regularization, in $x_2 = 0$ one obtains the set-valued function $F(x_1, 0)$ whose graph is plotted in Figure 6 b. Because the problem belongs to the class (1), it verifies the conditions in Theorem 1 and therefore a continuous selection can be found. If one approximate $sgn(x_2)$ with p_ε in a neighborhood of $x_2 = 0$, one obtains a smooth surface (Figure 6 c).

[5] Higher dimensional cases, such as R^3, are less common for discontinuous systems. However they can be treated similarly.

Thus, the discontinuous problem is transformed into the following continuous problem

$$\dot{x}_1 = x_2$$
$$\dot{x}_2 = \begin{cases} h_\varepsilon(x_1, x_2), & x_2 \in (-\varepsilon, \varepsilon), \\ -x_1 - sgn(x_2), & x_2 \notin (-\varepsilon, \varepsilon), \end{cases} \quad x_1 \in \mathbb{R}.$$

where $h_\varepsilon(x_1, x_2) = -x_1 - p_\varepsilon(x_2)$ and the OGY method applies as for continuous systems.

Conclusion In this paper we have proved that the OGY method for continuous systems can be applied to the class of systems modeled by the IVP (1). The possibility to used the generalized derivative, $\mathscr{D}_x$, introduced in Section 2, is the main fact which allows this implementation. The only restriction is to choose the Poincaré section different to the switching planes.

We saw that all steps of the method can be applied to (1). For this purpose, the existence of the necessary ingredients and the possibility of numerical implementation are proved.

Also, we proved that the IVP (1) can be continuously approximated by using the Cellina's Theorem. In this way, OGY method can be applied as for continuous systems.

References

1. Wiercigroch, M., de Kraker, B.: Applied Nonlinear Dynamics and Chaos of Mechanical Systems with Discontinuities. World Scientific, Singapore (2000)
2. Popp, K. Stelter, P.: Stick-slip vibrations and chaos. Philos. Trans. R. Soc. Lond. A **332**, 89-105 (1990)
3. Chillingworth, D.R.J.: Discontinuity geometry for an impact oscillator. Dynamical Systems **17**, 389420 (2002)
4. Cho, Y.-H., Pisano, A.P., Howe, R.T.: Viscous damping model for laterally oscillating microstructures. Journal of Microelectromechanical Systems **3**, 81 - 87 (1994)
5. Runesson, K., Ottosen, N.S., Dunja, P.: Discontinuous bifurcations of elastic-plastic solutions at plane stress and plane strain. International Journal of Plasticity, **7**, 99-121 (1991)
6. Govardham, R., Williamson, C.H.K.: Modes of vortex formation and frequency response of a freely vibrating cylinder. J. Fluid Mech. **420**, 85-130 (2000)
7. Salerno,M., Samuelsen, M.R., Filatrella, G., Pagano, S., Parmentier, R.D.: Microwave phase locking of Josephson-junction fluxon oscillators. Phys. Rev. B **41**, 66416654 (1990)
8. Sprott, J.C., Linz, S.J.: Algebraically Simple Chaotic Flows. International Journal of Chaos Theory and Applications **5**, 1-20 (2000)
9. Heemels, W.P.M.H., Çamlýbel, M.K., Schumacher, J.M.: On the Dynamic Analysis of Piecewise-Linear Networks. IEEE IEEE Trans. on Circ. & Syst. Part-I **49**, 315-327 (2002)
10. Sun, J., Mitchell, D.M., Greuel, M.F., Krein, P.T., Bass, R.M.: Averaged Modeling of PWM Converters Operating in Discontinuous Conduction Mode. IEEE Trans. Power Electron. **16**, 482-492 (2001)
11. Agrachev, A.A., Sachkov Y.L.: Control Theory from the Geometric Viewpoint. Springer Verlag, New York (2004)
12. Clarke, F.H.: Optimization and Non-smooth Analysis. Wiley-Interscience, New York (1983)
13. Barton, P.I., Allgor, R.J., Feehery, W.F., Galn, S: Dynamic Optimization in a Discontinuous Ind. Eng. Chem. Res. **37**, 966981 (1998)
14. Dasgupta, P. Maskin, E.: The Existence of Equilibrium in Discontinuous Economic Games, I: Theory. Review of Economic Studies **53**, 1-26 (1986)
15. Edwards, C. Spurgeon, S.K.: On the development of discontinuous observers. International Journal of Control **59**, 1211-1229 (1994)
16. De Santos, P.G., Jimenez, M.A.: Generation of discontinuous gaits for quadruped walking vehicles. Journal of Robotic Systems **12**, 599-611 (1995)
17. Mitchell, M.A., McRury, I.D., Everett, T.H., Li, H., Mangrum, J.M., Haines, D.E.: Morphological and physiological characteristics of discontinuous linear atrial ablations during atrial pacing and atrial fibrillation. Journal of Cardiovascular Electrophysiology **10**, 378-86 (1999)
18. Buhite, J.L., Owen, D.R.: An ordinary differential equation from the theory of plasticity. Arch. Rational Mech. Anal. **71**, 357-383 (1979)
19. Deimling, K. Multivalued differential equations, friction problems. Proc. Conf. Differential & Delay Equations, Ames, Iowa 1991: Fink, A.M., Miller, R. K., Kliemann, W. (eds.) pp. 99106. World Scientific, Singapore (1992)
20. Schilling, K.: An algorithm to solve boundary value problem for differential equations and applications in optimal control. Numer. Funct. Anal. Optim. **10**, 733-64 (1989)
21. Utkin, V.I.: Sliding regimes in optimization and control problems (in Russian). Nauka, Moscow (1981)
22. Ott, E., Grebogi, C., Yorke, A.: Controlling chaos. Phys. Rev. Lett. **64**, 1196-1199 (1990)
23. Güémez J, Matías M.A.: Control of chaos in unidimensional maps. Phys. Lett. A **181** 29-32 (1993)
24. Matías, M.A., Güémez, J.: Stabilization of chaos by proportional pulses in system variables. Phys. Rev. Lett. **72** 1455-1458
25. Danca, M.-F.: Controlling chaos in discontinuous dynamical systems. Chaos Solitons and Fractals **22**, 605-612 (2004)
26. Aubin, J.-P., Cellina, A.: Set-valued Maps and Viability Theory. Springer, Berlin (1984)
27. Aubin, J.-P. Frankowska, H.: Set-Valued Analysis. Vol.2 of Systems and Control: Foundations and Applications, Birkhäuser, Boston (1984)
28. Danca, M.-F.: Synchronization of Switch Dynamical Systems. Int. J. Bifurcat. Chaos **12**, pp. 1813-1826 (2002)
29. Filippov, A.F.: Differential Equations with Discontinuous Right-hand Sides. Kluwer Academic Publishers, Dordrecht (1988)
30. Danca, M.-F.: On a Class of Discontinuous Dynamical Systems. Mathematical Notes **2**, 103-116 (2001)
31. Dontchev, A. Lempio, F.: Difference Methods for Differentiale Inclusions: a Survey. SIAM Review **34**, 263-294 (1992)
32. Kastner-Maresch, A.: Implicit Runge-Kutta Methods for Differential Inclusions. Numer. Funct. Anal. and Optimiz. **10-11**, 937-958 (1991)
33. Parker, T.S., Chua, L.O. Practical Numerical Algorithms for Chaotic Systems. Springer-Verlag, New York (1989)
34. Colombo, A., di Bernardo, M., Hogan, S.J., Jeffrey, M.R.: Bifurcations of piecewise smooth flows: perspectives, methodologies and open problems. Physica D: Nonlinear Phenomena Available online 8 October (2011)

35. Leine, R.I., Van Campen, D.H., Van de Vrande, B.L.: Bifurcations in Nonlinear Discontinuous Systems. Nonlinear Dyn. **23**, 105164 (2000)
36. Diecia, L., Lopez,L.: Fundamental matrix solutions of piecewise smooth differential systems. Mathematics and Computers in Simulation **81**, 932953 (2011)
37. di Bernardo, M., Budd, C.J., Champneys, A.R., Kowalczyk, P., Nordmark, A.B., Tost, G.O., Piiroinen, P.T.: Bifurcations in Nonsmooth Dynamical Systems. SIAM Review **50**, 629-701 (2008)
38. di Bernardo, M., Kowalczyk, P. Nordmark, A.: Bifurcations of Dynamical Systems with Sliding: Derivation of Normal Form Mappings. Physica D **170**, 175-205 (2002)
39. Nusse, H.E., Yorke, J.A.: A procedure for finding numerical trajectories on chaotic saddles. Physica D **36**, 137-156 (1989)
40. England, J.P., Krauskopf, B., Osinga, H.M.:Computing One-Dimensional Global Manifolds of Poincaré Maps by Continuation. SIAM J. Appl. Dyn. Syst. **4**, 1008-1041 (2005)
41. Guckenheimer, J., Holmes, P.: Nonlinear oscillations, dynamical systems, and bifurcations of vector fields. Springer-Verlag, New York (1983)
42. Hénon, M.: On the numerical computation of Poincaré maps. Physica D, **5**, 412-414 (1982)
43. Tucker, W.: Computing accurate Poincaré maps. Physica D **171**, 127-137 (2002)
44. Palaniyandi, P.: On computing Poincaré map by Hnon method. Chaos, Solitons and Fractals **39**, 1877-1882 (2009)
45. Palis, J. de Melo, W.: Geometric Theory of Dynamical Systems. Springer-Verlag, Berlin (1982)
46. Kuznetsov, Y.A.: Elements of applied bifurcation theory. Springer, New York. (1995)
47. Lai, Y.-C., Grebogi, C., Yorke, J.A., Kan, I.: How often are chaotic saddles nonhyperbolic?. Nonlinearity **6**, 779-797 (1993)
48. Hsu, G.-H., Ott, E., Grebogi, C.: Strange saddles and the dimensions of their invariant manifolds. Phys. Lett. A **127**, 199-204 (1988)
49. Macau, E.E.N., Grebogi, C.: Control of chaos and its relevancy to spacecraft steering. Phys. Lett. A **127**, 199204 (2006)
50. Hobson, D.: An efficient method for computing invariant manifolds, Journal of Computational Physics **104** 14-22 (1991)
51. You, Z., Kostelich, E.J., Yorke, J.A.: Calculating stable and unstable manifolds. Int. J. Bifurc. Chao **1** 605-623 (1991)
52. Danca, M.-F., Codreanu, S.: On a possible approximation of discontinuous dynamical systems. Chaos Solitons and Fractals **13**, 681-691 (2002)
53. Andrievskii B.R., Fradkov, A.L.: Control of Chaos: Methods and Applications. I Methods. Automation and Remote Control **64** 673-713 (2003)

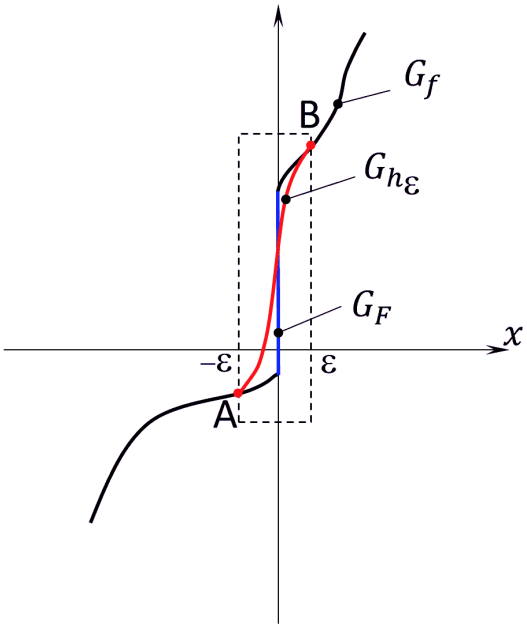

Fig. 1 Graph of an approximate selection h_ε in a ε-neighborhood of a set-valued function F (sketch).

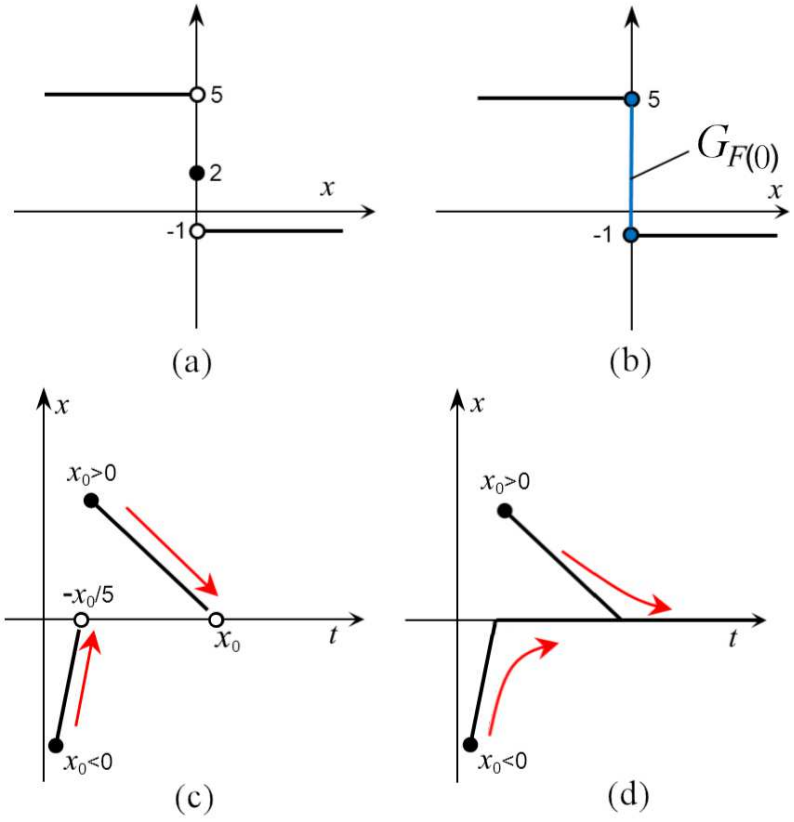

Fig. 2 Equation (4) (sketch). a) The right-hand side before regularization. b) The right-hand side after regularization. In $x = 0$, the discontinuity is replaced by the set-valued function $F(x)$. c) The solutions before regularization cannot be continued along the axis $x = 0$. d) After regularization, the problem admits generalized solutions defined on the entire axis $x = 0$.

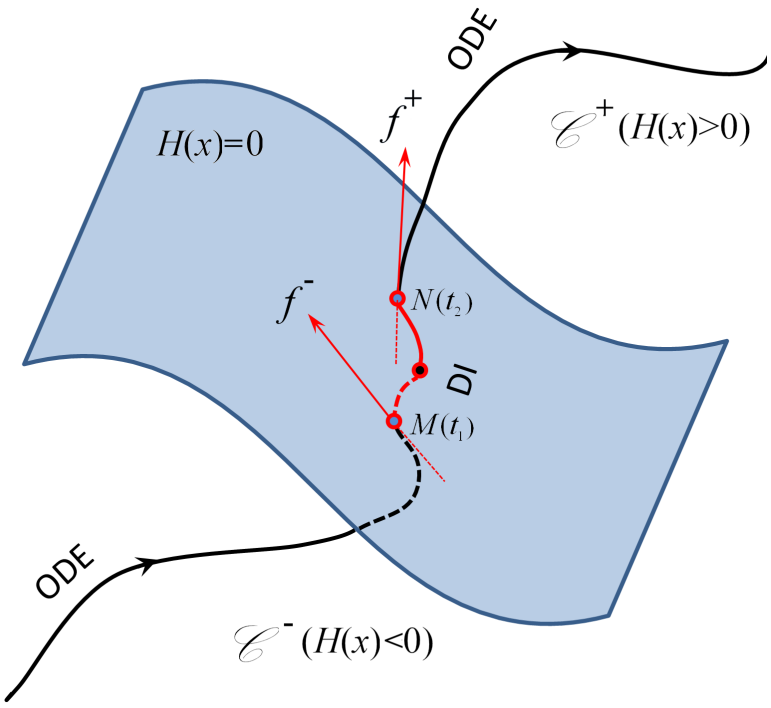

Fig. 3 A trajectory may have some corners when it transverses the switching surface, due to the different directions f^- and f^+ in the continuity domains $\mathscr{C}^-$ and $\mathscr{C}^+$ at the points M and N. In $\mathscr{C}^\pm$ the IVP is integrated as an ordinary ODE, while in $\mathscr{M}$ as a DI (sketch).

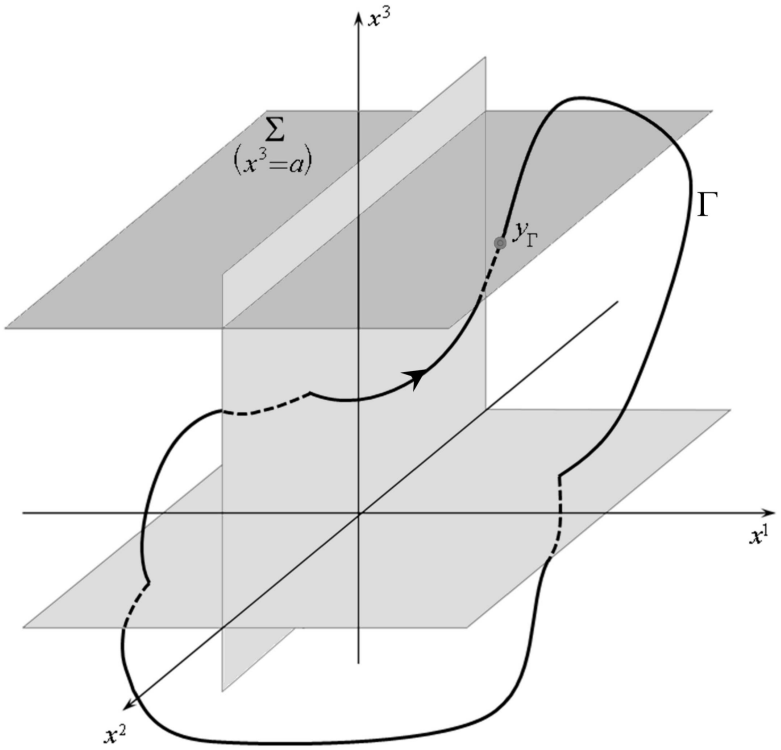

Fig. 4 Poincaré section and two switching surfaces.

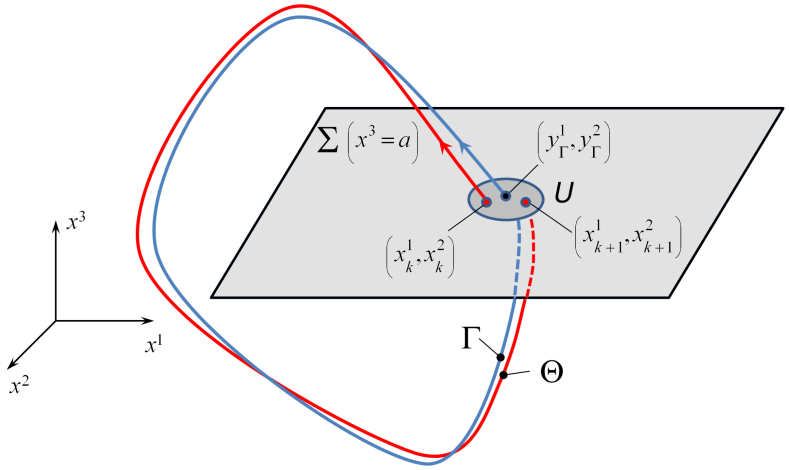

Fig. 5 Poincareé section and map (sketch).

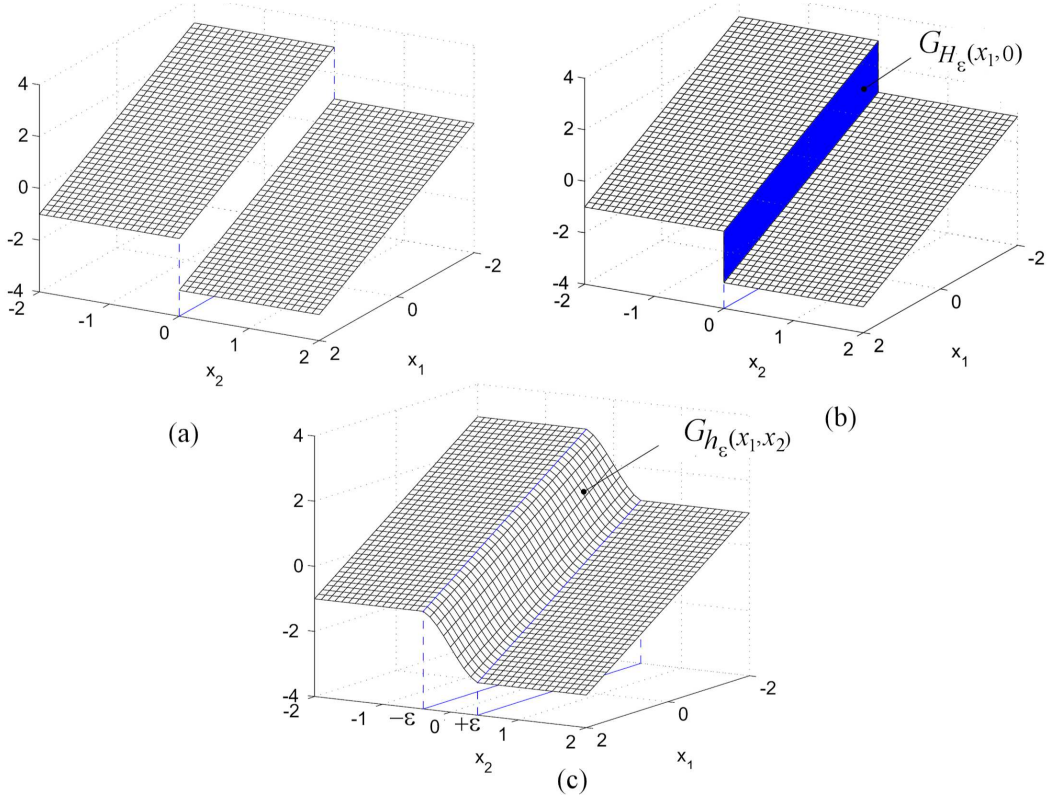

Fig. 6 Graph of the second component of the right-hand side of (17). a) Before regularization. b) After regularization in $x_2 = 0$, the graph of the set-valued function is a rectangular bounded surface. c) After the continuous approximation, the rectangular surface is replaced within an ε-neighborhood, with a continuous approximation.